Structural characterization and calorimetric dissolution behavior of Na2O-CuO-P2O5 glasses

Rachid Aït Mouss, Saida Krimi, Benoit Glorieux, Ismail Khattech, Michel Couzi, Thierry Cardinal, Abdelaziz El Jazouli

Structural characterization and calorimetric dissolution behavior of Na_2O–CuO–P_2O_5 glasses

Rachid Aït Mouss[a], Saida Krimi[a*], Benoît Glorieux[b], Ismail Khattech[c], Michel Couzi[d], Thierry Cardinal[b], Abdelaziz El Jazouli[e]

[a]*Laboratoire de Physico-Chimie des Matériaux Inorganiques, Faculté des Sciences Aïn-Chock, Université Hassan II Casablanca, B.P 5366, Maarif, Casablanca, Morocco*
[b]*Institut de Chimie de la Matière Condensée de Bordeaux, CNRS-Université de Bordeaux, 87 Av. Dr. Schweitzer, 33608 Pessac, France*
[c]*Laboratoire de Thermodynamique Appliquée, Faculté des Sciences de Tunis, Université de Tunis El Manar, Tunis, Tunisia*
[d]*Institut des Sciences Moléculaires, Université de Bordeaux, CNRS UMR 5255, Bâtiment A12, 351 cours de la libération, 33405 Talence cedex, France*
[e]*URAC17, Faculté des Sciences Ben M'Sik, Université Hassan II Casablanca, Av Driss El Harti, Casablanca, Morocco*

*Corresponding author. krimisaida@yahoo.fr

Abstract: Two series of glasses belonging to the ternary system Na_2O - CuO - P_2O_5 where copper is introduced differently were synthesized by the conventional melt-quenching technique. Both series start from meta-phosphate composition $NaPO_3$ ($50Na_2O$-$50P_2O_5$). In the first series, the Na_2O/P_2O_5 ratio is constant (Na_2O/P_2O_5 = 1) and both Na_2O and P_2O_5 oxides were replaced by copper oxide CuO: (50-*x*/2) Na_2O - *x*CuO - (50-*x*/2) P_2O_5, $0 \le x \le 40$. In the second series, the molar percentage of P_2O_5 is kept constant at 50 mol% and Na_2O is replaced by CuO: (50-*x*)Na_2O – *x*CuO – $50P_2O_5$, $0 \le x \le 50$. The glasses of these two series belong respectively to $NaPO_3$-CuO and $NaPO_3$-$Cu(PO_3)_2$ lines of the ternary system. These materials were characterized by density measurements, differential scanning calorimetry (DSC), X-ray diffraction (XRD), Raman, diffuse reflectance and dissolution heat measurements carried out with micro-calorimetry technique. Introduction of copper in meta-phosphate glass induces a blue/green color, and strengthens the vitreous network, as shown by the decrease of the molar volume (V_M) and the increase of the glass transition temperature (T_g) when the content of CuO rises. The crystallization of the glasses, followed by XRD, leads to the formation of $NaPO_3$, $Na_2CuP_2O_7$ or $Na_2Cu(PO_3)_4$ depending on the composition. Raman spectroscopy shows the conservation of the metaphosphate chains for $NaPO_3$-$Cu(PO_3)_2$ glasses characterized by a constant O/P ratio (O/P = 3) and the depolymerization of these chains for $NaPO_3$-CuO glasses where O/P ratio varies from 0 to 3.67. UV - visible study showed that the optical energy gap decreases by increasing the CuO concentration. Calorimetric study of the dissolution of glasses in acid solution shows a decrease of the dissolution enthalpy, for both series, when the CuO content increases. The dissolution phenomenon is endothermic for glasses with low content in CuO ($x < 30$) and exothermic for glasses rich in CuO.

Keywords: Sodium copper phosphate ; Glasses ; Density ; DSC ; XRD ; Raman ; UV-visible ; Heat of dissolution

1. Introduction

It is known that phosphate glasses have become of great interest in recent times thanks to their specific physical and chemical unique properties that imply very different applications. We can name among these interesting properties the following: low glass transition temperatures, low melting and softening temperatures, high electrical conductivity and interesting dielectric properties [1], large thermal expansion coefficients [2], and also high optical transparency window over the UV, visible and infrared wavelength range [3]. All these properties make phosphate glasses interesting and useful materials candidates for a wide range of technical applications such as: high power laser devices [4], solid

electrolytes [5], biomaterials for neural repair [6], tissue engineering [7], [8], and bone fracture fixation [9]. However, glass technologists for a long time bypassed pure phosphate glasses because they usually have a relatively poor chemical durability in aqueous solutions. This major disadvantage is caused by the easily hydrolysable P—O—P bonds that are setup by the network former oxide P_2O_5 inside the glassy matrix. For this reason the addition of at least one network forming or modifying oxide as Al_2O_3, Ga_2O_3, Fe_2O_3, PbO, SnO, ZnO, etc., is suggested in order to overcome this weakness by providing more covalent bonds resistant to water attack [10]. The diverse properties and applications of phosphate glasses depend on their structure, which is based on the distribution of Q^n tetrahedral units in the vitreous network (n varies from 0 to 3 and represents the number of bridging oxygen per PO_4 tetrahedron). Connection of PO_4 tetrahedra gives rise to different phosphate groups depending on the value of O/P ratio. So, the glass structure can be formed by a cross-linked network of Q^3 tetrahedra (vitreous P_2O_5, O/P = 2.5), infinite metaphosphate chains of Q^2 tetrahedra (vitreous $NaPO_3$, O/P = 3), or by small diphosphate $P_2O_7^{2-}$ (Q^1, O/P = 3.5) and monophosphate PO_4^{3-} (Q^0, O/P = 4) anions [11].

The oldest work on sodium copper phosphate glasses dates back to 1969, when Maekawa et al. studied the optical spectra and magnetic susceptibilities of different transition metal oxides in vitreous $NaPO_3$. They concluded that most Cu^{2+} ions coordinate six oxygen atoms in the copper phosphate glasses [12]. Since then, many other studies have been conducted on glasses belonging to the ternary system Na_2O—CuO—P_2O_5. The glass formation zone of this system has been identified and studied with various characterization techniques. Thermal analysis has been performed by Differential Thermal Analysis (DTA) and showed that when replacing Na_2O by CuO, the glass transition temperature T_g increases. Also according to dilatometry measurements the softening temperature T_d and hardness are found to increase as the copper content increases, while the thermal expansion coefficient decreases. FTIR and XPS analysis suggest that the modification occurring on the structure can be explained by the formation of POCu bonds, which replace P—O—P and P—O—Na bonds. These new formed bonds are greatly influenced by the experimental conditions of the glass melting; indeed increasing melting time and melting the mixture in flowing oxygen atmospheres instead of air enhance this phenomenon. ^{31}P magic angle spinning nuclear magnetic resonance (MAS-NMR) spectroscopy showed that the phosphate chain length is shortened as the CuO content increases and that the formation of P—O—Cu bonds is easier in the polyphosphate glasses than in metaphosphate ones. FTIR and Raman spectroscopies confirmed the structure of phosphate species i.e. the infinite metaphosphate chains get depolymerized by addition of CuO. Simulation of EPR spectra of (50-*x*/2) Na_2O–*x*CuO–(50-*x*/2) P_2O_5 ($0 \leq x \leq 30$) glasses showed that Cu^{2+} ions occupy two sites: one of them is preponderant at low Cu content and the other is preponderant at high content of Cu. EPR parameters of site at low content are consistent with Cu^{2+} in an elongated octahedron. However, the values of the orbital reduction factors, deduced from EPR and optical data, are consistent with Cu^{2+} surrounded by four ligands [13], [14], [15], [16], [17], [18].

In this paper, we report on two different series of glasses belonging to the ternary system Na_2O-CuO-P_2O_5: (50-*x*/2) Na_2O - *x*CuO - (50-*x*/2) P_2O_5 ($0 \leq x \leq 40$) and (50-*x*)Na_2O - *x*CuO - 50P_2O_5, ($0 \leq x \leq 50$) with x is the molar percent or [(0.5-x/2)Na_2O-xCuO-(0.5-x/2)P_2O_5 ($0 \leq x \leq 0.4$) and (0.5-*x*)Na_2O - *x*CuO – 0.5P_2O_5, ($0 \leq x \leq 0.5$)] with x is molar fraction. The aim of the study is to investigate the evolution of the glass matrix structure, while introducing CuO, by different characterization methods: density measurements, Differential scanning calorimetry (DSC), X-ray diffraction (XRD), Raman and diffuse reflectance spectroscopies, and micro-calorimetry.

2. Materials and experimental procedures

2.1. Glass samples preparation

Analytical grade powders of sodium carbonate Na_2CO_3 (99%, Sigma Aldrich), copper oxide CuO (98%, Merck) and ammonium dihydrogen phosphate $NH_4H_2PO_4$ (99%, Merck), were used as starting materials. The chemicals in appropriate amounts were thoroughly hand mixed in a porcelain mortar to obtain a homogenized mixture. The mixtures were subjected first to heat treatments between 200 and 600 °C, in a muffle furnace, to eliminate volatile species NH_3, H_2O and CO_2. They were then melted in a platinum crucible, at temperatures within a range from 750 °C to 1050 °C depending on the glass composition, for about 30 min. The melts were then quenched to room temperature in air. Vitreous $NaPO_3$ is colorless while glasses containing copper are colored. The color varies from blue to green (Fig. 1). After the preparation, each glass is annealed at T_g-20 °C, to remove internal stresses, and then stored in a desiccator in order to minimize water absorption. The crystallization of the synthesized glasses was done by heating bulk vitreous samples at their corresponding T_g + 40 °C temperature for 12 h. The obtained crystalline materials were ground and analyzed by XRD.

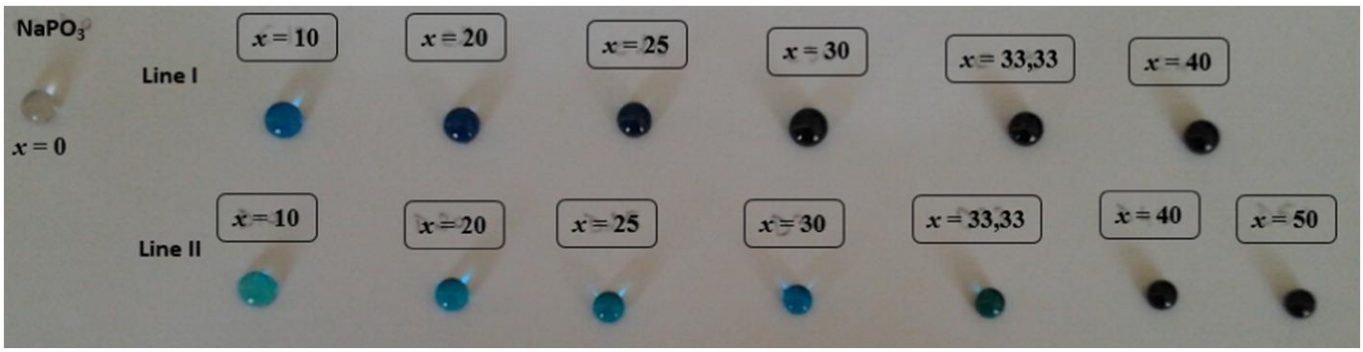

Fig. 1. Photographs of (50-x/2) Na_2O – xCuO – (50-x/2) P_2O_5 ($0 \leq x \leq 40$) and (50-x) Na_2O – xCuO – 50 P_2O_5 ($0 \leq x \leq 50$) glasses showing the evolution of the color versus CuO content.

2.2. Characterization of the glasses

X-ray diffraction (XRD) measurements were done at room temperature with a powder diffractometer (PANalytical X'Pert Pro) using Cu Kα radiation. Data was collected from 10° to 70° 2θ with a step of 0.02 and a count time of 12 s.

The density (ρ) of each glass was determined by the Archimedes method using diethyl phthalate as immersion liquid. Three samples of each composition were analyzed and the average density is reported. The accuracy of the density measurements is about ± 0.03 g cm^{-3}. The molar volume (V_M = M/ρ) of glasses was calculated from the density (ρ) and the molar mass (M) and its random error was retrieved considering the accuracy of the density measurements.

Differential Scanning Calorimetry (DSC) was used to determine the transition and crystallization temperatures (T_g, T_c). DSC curves of powders (30–40 mg), obtained by crashing the glasses, were recorded on a computerized system (DSC 404 PC from Netzsch Inc.), from ambient temperature to 600 °C, at a heating rate of 10 °C/min. The instrumental error of all measured values is ± 5 °C. The measurements were carried out in hermetically sealed aluminum pans. The glass transition temperature (Tg) was taken as the inflection point of the endothermic peak and the crystallization temperature (Tc) at the maximum of the exothermic peak.

The Raman spectra of the vitreous samples were recorded on a confocal micro-Raman Labram (Horiba/Jobin-Yvon) spectrophotometer with a backscattering mode at room temperature in the range 250–1400 cm^{-1}. The excitation source was a 532 nm continuous laser. A holographic Notch filter was used to reject the Rayleigh diffusion. The backscattered light was collected through a 100 × objective and selectively transmitted toward a cooled CCD detector.

The dissolution heat of the samples was measured on a Setaram Calvet C-80 μ-calorimeter. This latter is composed by a reference cell containing only the solvent, and a working cell which comprises an inferior compartment, receiving an amount of approximately 20 mg of the ground glass sample, and a superior compartment where 4.5 ml of the acid solution were introduced. These two compartments are separated by a metallic lid, which opens when the reaction starts and allows contact between the material and the attacking solution. Both of the cells are surrounded by high performance thermopiles allowing the detection of the heat flow that resulted from the dissolution of different samples of solids. The dissolution reaction of the vitreous powder samples in a nitric acid solution (9 wt%) was carried out at a fixed temperature (25 °C). The dissolution enthalpy was determined by integrating the surface of the raw signal taking into account the calibration coefficient which was determined in previous works [19], [20]. The accuracy on those measurements was calculated using statistical model proposed by Pattengill [21]. The random error of the dissolution heat was calculated considering five integrations of raw signal of the dissolution.

Diffuse reflectance spectra were recorded on powders, obtained by crushing the glasses, in the 250–750 nm range, using a spectrofluorimeter SPEX FL212 with a 450 W xenon lamp light source. The reflectance is measured in a synchronous mode and compared to black (toner powder) and white (MgO) references. The measurements were confirmed on selected samples by direct transmittance measurements obtained on a Carry-Varian 5000 performed on thin polished glasses.

3. Results and discussion

Two compositional series of sodium copper phosphate glasses were prepared and studied (Fig. 2). Line **(I)** represents the compositions $(50\text{-}x/2)Na_2O - xCuO - (50\text{-}x/2)\ P_2O_5$ $(0 \le x \le 40)$ where CuO is added to $NaPO_3$, x = 0 corresponds to the metaphosphate $NaPO_3$ and $x = 33.33$ corresponds to the diphosphate $Na_2CuP_2O_7$. An attempt to synthesize the glass with composition $25Na_2O - 50CuO - 25P_2O_5$ ($NaCuPO_4$) was done, but it led to a crystalline product. Line **(II)** represents the compositions $(50\text{-}x)\ Na_2O - xCuO - 50P_2O_5$ $(0 \le x \le 50)$ located between the two metaphosphate extremities $NaPO_3$ and $Cu(PO_3)_2$ with the composition $Na_2Cu(PO_3)_2$ (x = 25) in between. Table 1 summarizes the major interesting measured properties for all studied vitreous materials. All vitreous samples prepared were confirmed to be amorphous using XRD analysis. As seen in Fig. 3, the glassy behavior shows a broad hump at 2θ = 30–33°. No peak corresponding to any crystalline material is observed. This indicates that all components have completely entered the glassy matrix.

Table 1
Nominal molar compositions, colors, molar masses, densities, molar volumes, and characteristic temperatures of $(50\text{-}x/2)Na_2O - xCuO - (50\text{-}x/2)P_2O_5$ $(0 \le x \le 40)$ and $(50\text{-}x)Na_2O - xCuO - 50P_2O_5$ glasses $(0 \le x \le 50)$.

Molar compositions (mol%)			Color	O/P	Molar mass ($g.mol^{-1}$)	Density ($g.cm^{-3}$) (±0.03)	Molar volume ($cm^3.mol^{-1}$)	T_g (°C) (±5)	T_c (°C) (±5)
Na_2O	CuO	P_2O_5							
50	0	50	Colorless	3	101.96	2.47	41.3 ± 0.5	280	290
Line I: $(50\text{-}x/2)\ Na_2O - x\ CuO - (50\text{-}x/2)\ P_2O_5$									
45	10	45	Light blue	3.11	99.72	2.64	37.8 ± 0.5	301	450
40	20	40	Blue	3.25	97.48	2.81	34.7 ± 0.4	314	480
37.5	25	37.5	Dark blue	3.33	96.36	2.9	33.2 ± 0.4	328	485
35	30	35	Dark blue	3.43	95.23	3.02	31.5 ± 0.4	350	489
33.33	33.33	33.33	Dark blue	3.5	94.48	3.1	30.5 ± 0.3	364	477
30	40	30	Dark blue	3.67	92.99	3.26	28.5 ± 0.3	368	504
Line II: $(50\text{-}x)\ Na_2O - x\ CuO - 50\ P_2O_5$									
40	10	50	Light cyan	3	103.72	2.59	40.1 ± 0.5	292	-
30	20	50	Sky blue	3	105.47	2.68	39.4 ± 0.5	298	523
25	25	50	Sky blue	3	106.35	2.77	38.4 ± 0.5	300	503
20	30	50	Sky blue	3	107.23	2.82	38.0 ± 0.4	311	550
16.67	33.33	50	Dark cyan	3	107.81	2.87	37.6 ± 0.4	346	491 and 564
10	40	50	Dark green	3	108.98	2.93	37.2 ± 0.4	390	546
0	50	50	Dark green	3	110.74	3.11	35.7 ± 0.4	460	–

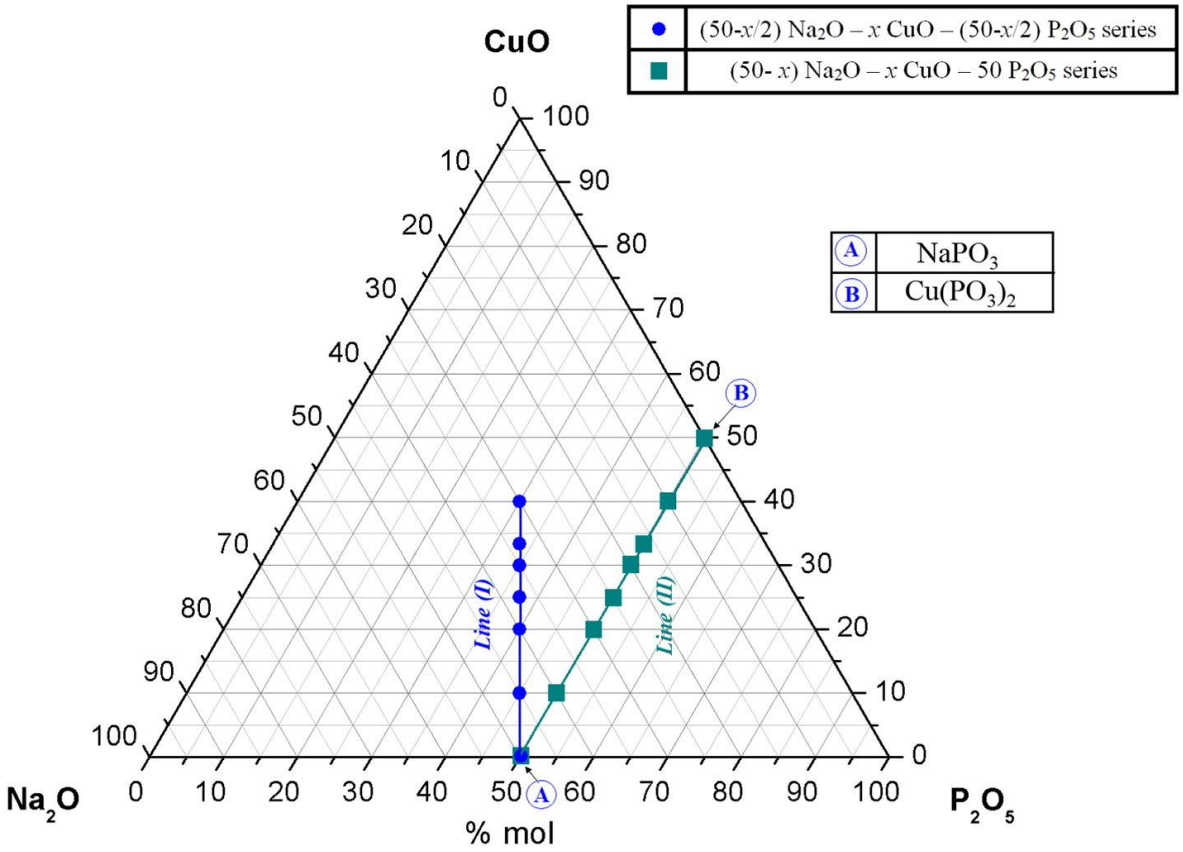

Fig. 2. Compositions of (50-x/2)Na_2O – xCuO – (50-x/2)P_2O_5 ($0 \leq x \leq 40$) (line I) and (50-x)Na_2O – xCuO – 50P_2O_5 ($0 \leq x \leq 50$) (line II) glasses in the Na_2O – CuO – P_2O_5 ternary diagram.

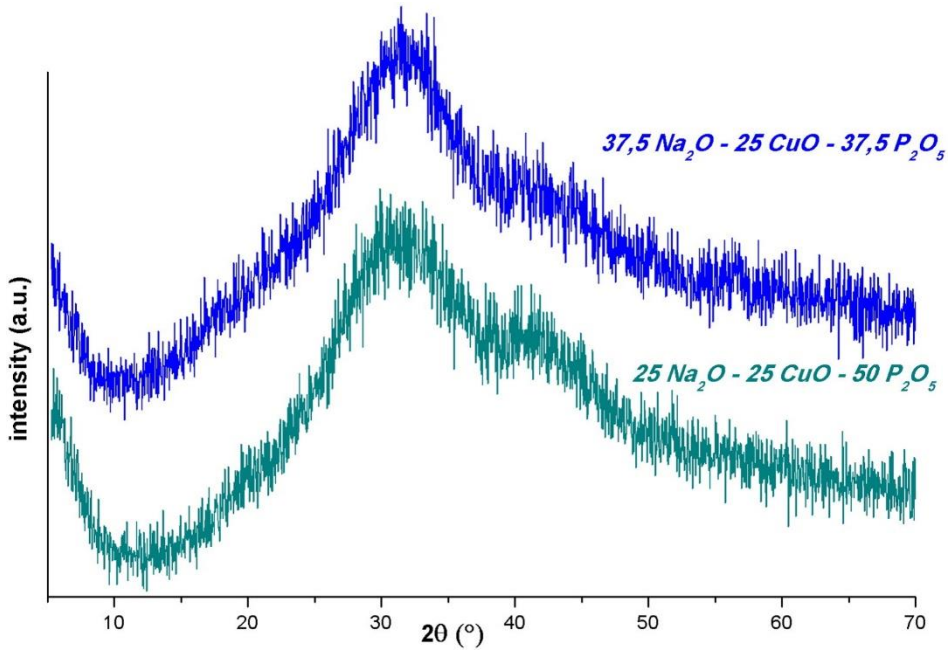

Fig. 3. X-ray diffraction spectra of two glasses of Na_2O – CuO – P_2O_5 system.

3.1. Density and molar volume

Fig. 4 shows the variation of the molar mass (M), the density (ρ) and the molar volume (V_M) versus CuO content, for both series of glasses. The molar mass M (M = xM(Na_2O) + yM(CuO) + zM(P_2O_5), with the

molar fractions sum x + y + z = 1) decreases for (50-*x*/2)Na_2O – *x*CuO – (50-*x*/2)P_2O_5 ($0 \le x \le 40$) glasses and increases for (50-*x*) Na_2O – *x*CuO – 50 P_2O_5 ($0 \le x \le 50$) glasses, while the density increases and the molar volume decreases for both series, when CuO content rises. The variation of the molar volume is less important for the second series due to the increase of the molar mass of the glasses of this series (Table 1). The reticulation of the glass network induced by the decrease of the molar volume for both series of glasses is due to the replacement of Na—O bonds by the more covalent Cu—O bonds. The evolution of molar volume and density are in agreement with the results obtained by Chahine et al. [17].

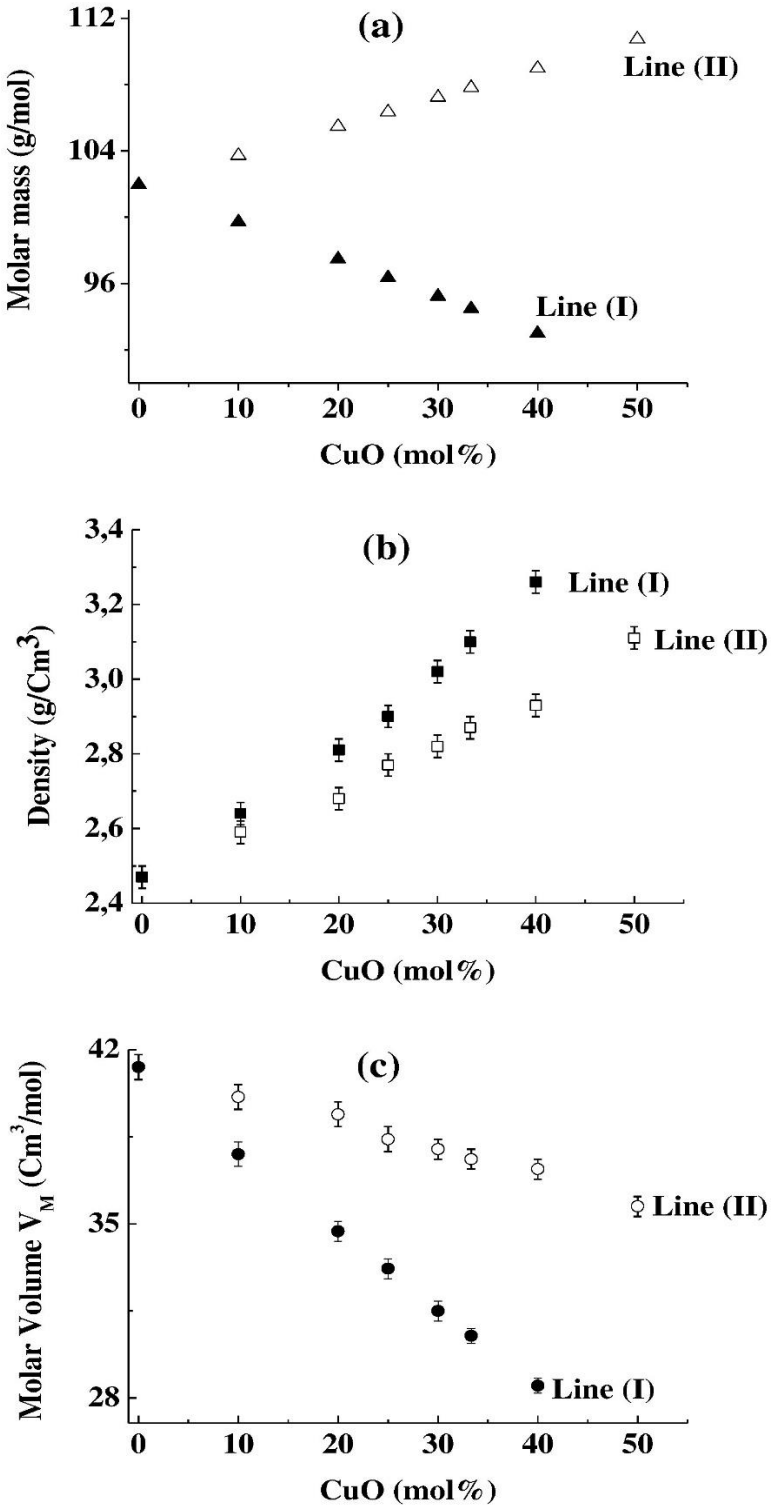

Fig. 4. Evolution of molar mass (a), density (b), and molar volume (c) for (50-x/2)Na_2O–xCuO–(50-x/2)P_2O_5 (Line (I)) ($0 \le x \le 40$) and (50-x)Na_2O–xCuO–50P_2O_5 (Line (II))($0 \le x \le 50$) glasses versus CuO mol%.

3.2. Thermal analysis data

DSC thermograms are shown in Fig. 5, Fig. 6 respectively for (50-*x*/2)Na_2O-*x*CuO-(50-*x*/2) P_2O_5 ($0 \leq x \leq 40$) and (50-*x*) Na_2O - *x*CuO - 50 P_2O_5 ($0 \leq x \leq 50$) glasses. Fig. 7 shows the behavior of the glass transition temperature as a function of CuO concentration in both series. The results are summarized in Table 1. For the glasses of the first series, T_g increases regularly from 280 °C (x = 0) to about 364 °C with increasing CuO content up to x = 33.33, and then increases slowly up to 368 °C for x = 40. For the glasses of line (II) T_g increases from 280 °C (x = 0) to 311 °C (x = 30) and then increases very rapidly up to 460 °C for 50 mol% CuO content. For a same composition of CuO, T_g values for glasses of the first series are superiors to those of the second series, in the range 0 ≤ mol% CuO ≤ 33.33. After, the glasses of the second series become more thermally stable with higher values of T_g. The increase of glass transition temperature values shows that the introduction of copper oxide (CuO) in the metaphosphate glass strengthens the vitreous network. This observation confirms the previous results obtained for densities and molar volume measurements regarding the reticulation of the glass system and therefore its stability. A similar behavior was observed for other phosphate glasses containing Zn^{2+}, Mn^{2+}, Mg^{2+} or Sr^{2+} ions. Glass transition temperature increases from 280 °C (x = 0) to: 314 °C (Zn^{2+}, x = 33%) [22], 402 °C (Mn^{2+}, x = 33%) [23], 449 °C (Mg^{2+}, x = 43%) [24] and 323 °C (Sr^{2+}, x = 20) [25] in [(100-x) $NaPO_3$ – *x*MO]. When metal oxide (MO) is incorporated, the structure strengthened because ionic NaO bonds are replaced by covalent bond M—O allowing the compactness of vitreous network. As a result there is an increase in the glass transition temperature.

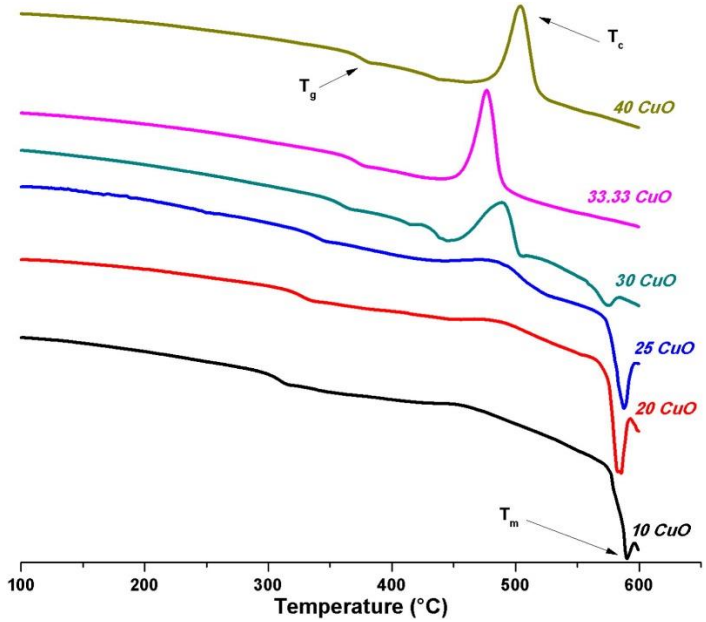

Fig. 5. DSC thermograms for (50-x/2) Na_2O – x CuO – (50- x/2) P_2O_5 ($0 < x \leq 40$) glasses.

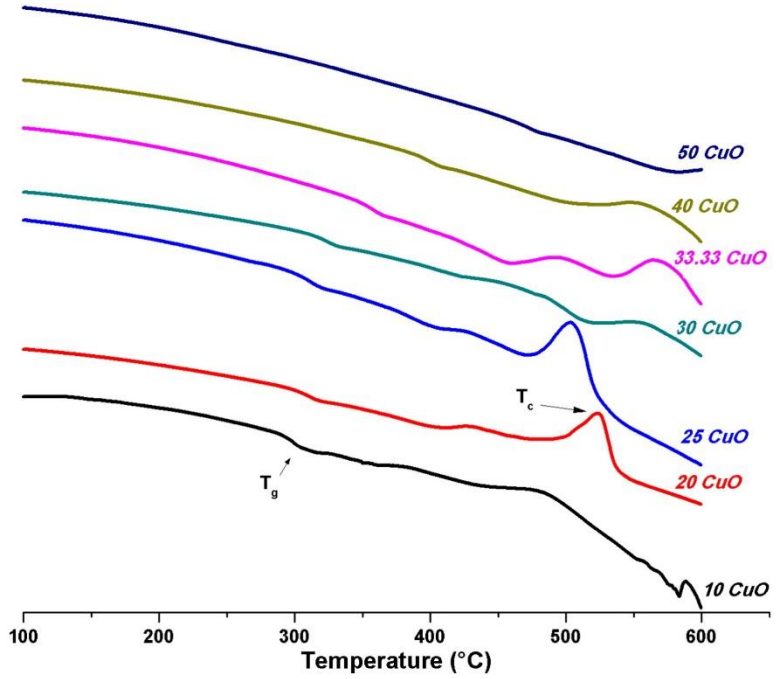

Fig. 6. DSC thermograms for (50-x) Na_2O – x CuO – 50 P_2O_5 (0 < x ≤ 50) glasses.

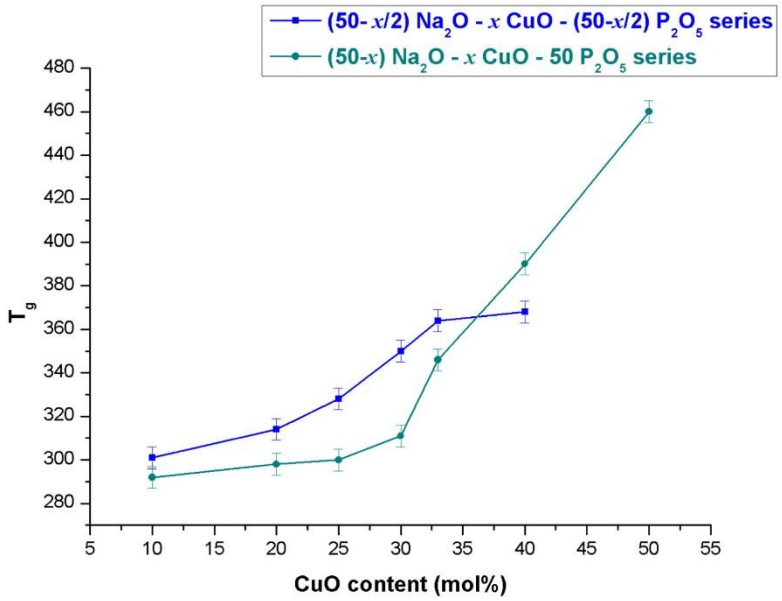

Fig. 7. Variation of glass transition temperature versus CuO content for (50-x/2) Na_2O – x CuO – (50-x/2) P_2O_5 (0 < x ≤ 40) and (50-x) Na_2O – x CuO – 50 P_2O_5 (0 < x ≤ 50) glasses. The lines are drawn as guide to the eyes.

3.3. Crystallization of the glasses

Fig. 8, Fig. 9 show some XRD patterns, as examples, respectively for (50-*x*/2)Na_2O – *x*CuO – (50-*x*/2) P_2O_5 (x = 20 and 33.33%) and (50-*x*)Na_2O – *x*CuO – 50P_2O_5 (x = 20 and 25%) glasses heated at T_g + 40 (°C) for 12 h. The identified crystalline phases from the annealed glasses are shown in Table 2. The crystallization of (50-*x*/2)Na_2O – *x*CuO – (50-*x*/2)P_2O_5 glasses with 0 ≤ x ≤ 30, leads to the formation of both $NaPO_3$[26] and $Na_2CuP_2O_7$[27] crystalline phases. For glass compositions with x ≥ 33.33, we observe mainly the crystallization of the diphosphate $Na_2CuP_2O_7$. One notices that $NaPO_3$ phase disappeared for 33.33Na_2O–33.33CuO–33.33P_2O_5 ($Na_2CuP_2O_7$) composition, indicating that at this level all metaphosphate chains were depolymerized into diphosphate groups. Crystallization of (50-*x*)Na_2O – *x*CuO – 50P_2O_5 (0 < x < 50)

glasses leads to the formation principally of $Na_2Cu(PO_3)_4$[28] meta-phosphate phase together with some unidentified peaks (Fig. 9). Glasses of compositions $10Na_2O$ - 40CuO - $50P_2O_5$ and 50CuO - $50P_2O_5$ heated at their T_g + 40 °C temperatures remains amorphous.

Table 2
Identified crystalline phases in the corresponding annealed glasses at ~T_g + 40 (°C). (NIP: Non-identified peaks).

Molar compositions (mol%)			Annealing temperature (°C)	Identified crystalline phases
Na_2O	CuO	P_2O_5		
45	10	45	341	$NaPO_3$ + β-$Na_2CuP_2O_7$
40	20	40	354	$NaPO_3$ + β-$Na_2CuP_2O_7$ + α-$Na_2CuP_2O_7$
37.5	25	37.5	368	$NaPO_3$ + β-$Na_2CuP_2O_7$ + α-$Na_2CuP_2O_7$ + NIP
35	30	35	390	β-$Na_2CuP_2O_7$ + $NaPO_3$
33.33	33.33	33.33	404	β-$Na_2CuP_2O_7$
30	40	30	408	β-$Na_2CuP_2O_7$ + NIP
40	10	50	332	$NaPO_3$ + $Na_2Cu(PO_3)_4$ + NIP
30	20	50	338	$Na_2Cu(PO_3)_4$ + NIP
25	25	50	340	$Na_2Cu(PO_3)_4$
20	30	50	351	$Na_2Cu(PO_3)_4$ + NIP (still partially amorphous)
16.67	33.33	50	386	$Na_2Cu(PO_3)_4$ + NIP (still partially amorphous)
10	40	50	430	Amorphous
0	50	50	500	Amorphous

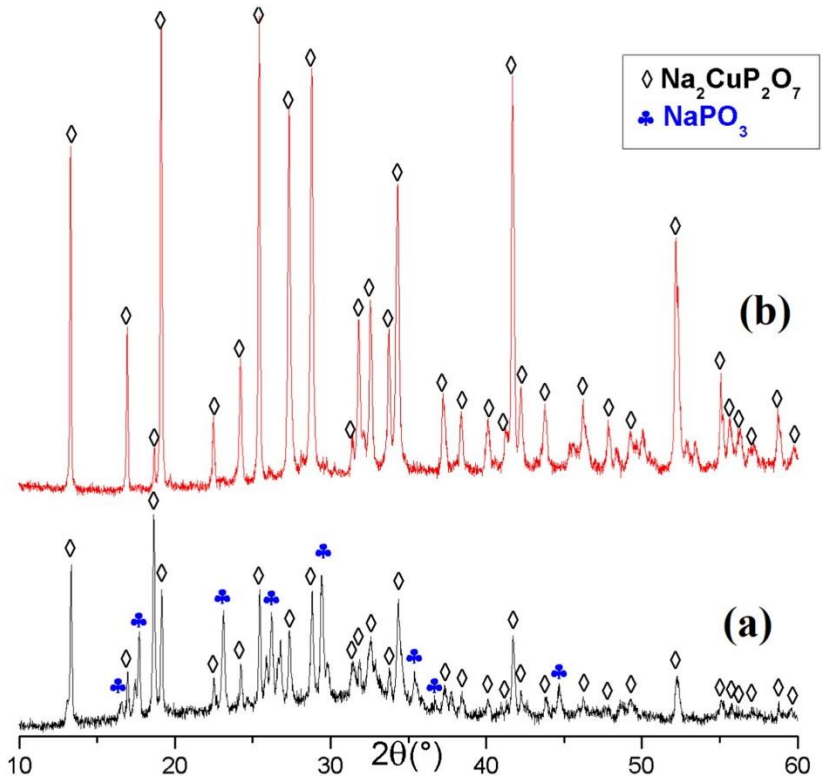

Fig. 8. X-ray diffraction patterns for glasses heated at T_g + 40 °C: (a) $40Na_2O – 20CuO – 40 P_2O_5$ (b) $33.33 Na_2O – 33.33CuO – 33.33P_2O_5$.

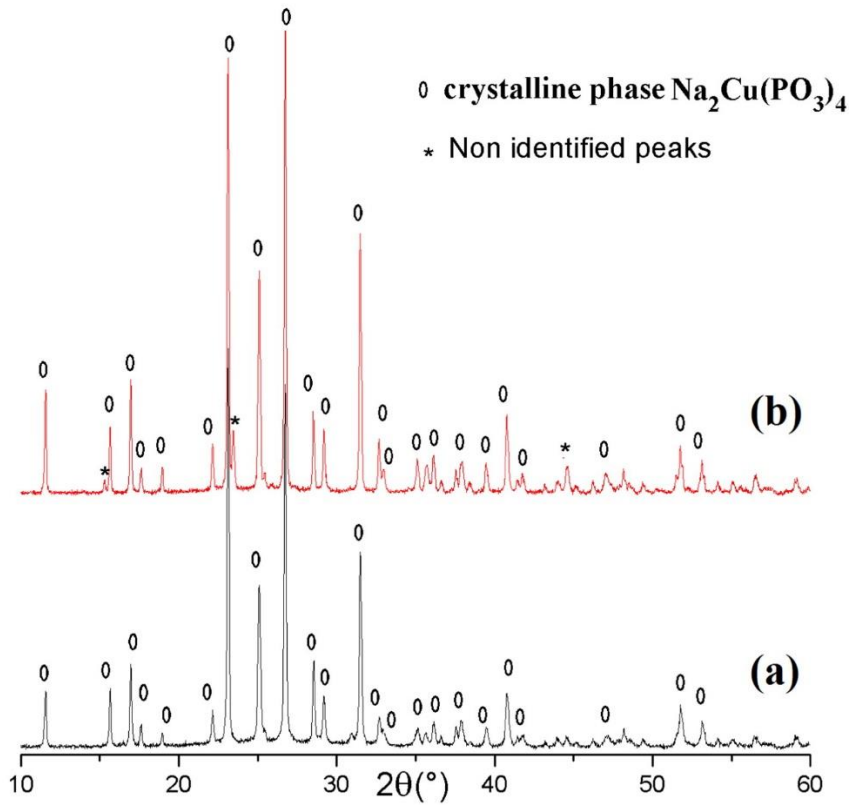

Fig. 9. X-ray diffractograms for glasses heated at T_g + 40 °C; (a) 25Na_2O – 25CuO – 50 P_2O_5 (b) 30 Na_2O – 20CuO – 50 P_2O_5.

3.4. Raman spectroscopy

Fig. 10, Fig. 11 show the experimental Raman spectra respectively for (50-*x*/2)Na_2O – *x*CuO – (50-*x*/2)P_2O_5 (0 ≤ *x* ≤ 40; line I) and (50-*x*)Na_2O – *x*CuO – 50P_2O_5 (0 ≤ *x* ≤ 50; line II) glasses. Table 3 summarizes the most important bands and their assignments.

As expected, the Raman spectra of the mixed $NaPO_3$-$Cu(PO_3)_2$ glasses (O/P = 3) corresponding to line (II) (Fig. 11) are dominated by the bands characteristic of glasses with metaphosphate composition, i.e. the strong bands at ~ 1170 cm^{-1} due to the symmetric stretching mode of the PO_2 middle groups $\nu_s(PO_2)$ and at ~ 685 cm^{-1} due to the symmetric stretching mode of the P-O-P bridges $\nu_s(POP)$ [17], [28].

Note also in all spectra the presence of a band near 1270 cm^{-1} attributed to the asymmetric stretching mode of the PO_2 middle groups $\nu_{as}(PO_2)$ [29]. It is known that the structure of the $Na_2Cu(PO_3)_2$ crystalline phase corresponding to the glass composition x = 25 is made of infinite metaphosphate chains [28], whereas the crystal with composition $Cu(PO_3)_2$ (x = 50) is made of four membered P_4O_{12} cyclic units, i.e. it is more precisely described by the formula $Cu_2P_4O_{12}$[30]. Furthermore, a ^{31}P MAS-NMR study of this series of glasses has shown that for high Cu contents, the glass contains both – O– PO_2– O (denoted as $Q^{(2)}$)

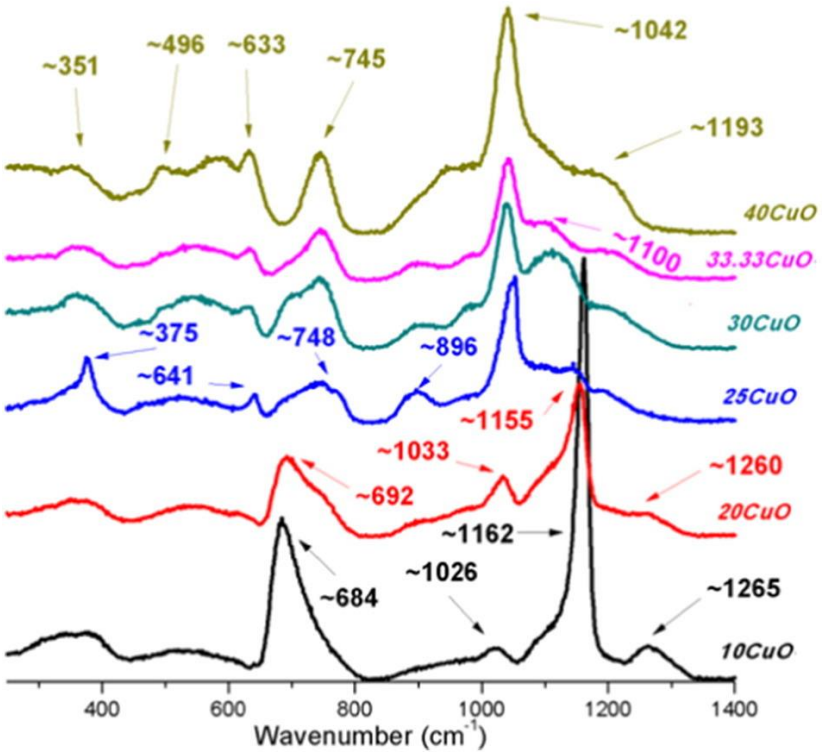

Fig. 10. Raman spectra of (50-x/2) Na_2O – x CuO – (50- x/2) P_2O_5 (0 < x ≤ 40) glasses.

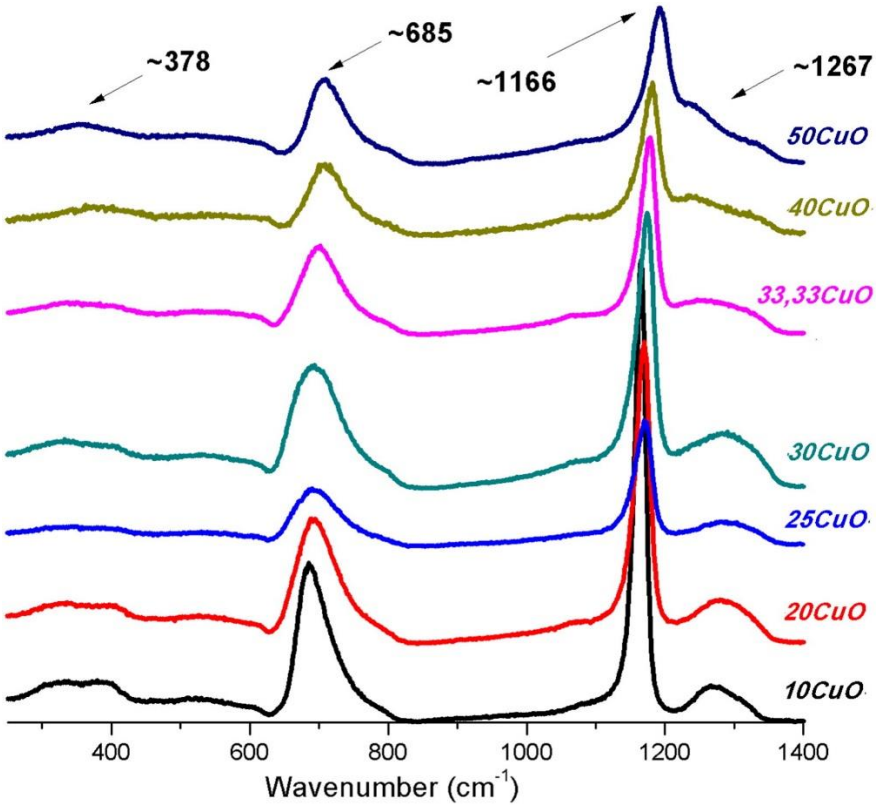

Fig. 11. Raman spectra of (50-x) Na_2O – x CuO – 50 P_2O_5 (0 < x ≤ 50) glasses.

middle groups and –O–PO_3 (denoted as $Q^{(1)}$) end groups [16]. Note that the $Q^{(2)}$ species bear a charge of − 1 and the $Q^{(1)}$ ones bear a charge of − 2. Obviously, this is not compatible with the chain nor with the cyclic metaphosphate structural units that contain $Q^{(2)}$ species only. In order to conciliate the

simultaneous presence of $Q^{(1)}$ and $Q^{(2)}$ species in a glass with a global metaphosphate composition, we suppose that charge equilibrium is realized by the presence of neutral "branching" groups O = $PO_{3/2}$ (denoted as $Q^{(3)}$), such as those found in P_2O_5 and in the ultra-phosphates, according to the scheme: $2Q^{(2)} \leftrightarrow Q^{(1)} + Q^{(3)}$. Indeed, in the glasses with high Cu contents ($33.33 \leq x \leq 50$) two broad shoulders develop progressively on each side of $v_s(PO_2)$, situated at ~ 1320 cm^{-1} and ~ 1050 cm^{-1} that we assign respectively to the stretching vibration v(PO) of the branching units $Q^{(3)}$ and to the symmetric stretching vibration $v(PO_3)$ in $Q^{(1)}$ end groups, respectively (Table 3). The presence of $Q^{(1)}$ and $Q^{(3)}$ species may also be due to slight departures of the experimental compositions from the metaphosphate composition, but they are not expected to be present simultaneously, since charge compensation would not be necessary in those cases. Therefore, we conclude that the presence of high CuO contents in meta-phosphates (line II) provokes a partial depolymerization of the phosphate chains, thus creating PO_3 end groups compensated by the creation of $Q^{(3)}$ branching groups between chain fragments, thus insuring the reticulation of the glass network and providing new P═O terminal sites, probably to accommodate a distorted octahedral environment of oxygen atoms around the Cu^{2+} ions [28], [30].

Table 3
Raman band assignments of $(50\text{-}x/2)Na_2O - xCuO - (50\text{-}x/2)P_2O_5$ $(0 < x \leq 40)$ and $(50\text{-}x)Na_2O - xCuO - 50P_2O_5$ $(0 < x \leq 50)$ glasses.

Wavenumber (cm^{-1})	Band assignment
~350	Bending vibrations of phosphate polyhedral.
~630	Symmetric stretch of $CuO_{4/2}$ units (Cu-O-P bridges)
~685	POP symmetric stretch of metaphosphate and polyphosphate chains ($Q^{(2)}$).
~745	POP symmetric stretch of pyrophosphate groups ($Q^{(1)}$).
~1050	Symmetric stretch of PO_3 end groups in polyphosphate chains and pyrophosphate groups ($Q^{(1)}$).
~1170	Symmetric stretch of PO_2 middle groups in metaphosphate and polyphosphate chains ($Q^{(2)}$)
~1260	Antisymmetric stretch of PO_2 middle groups in metaphosphate and polyphosphate chains ($Q^{(2)}$)
~1320	P = O stretch of O = $PO_{3/2}$ branching units ($Q^{(3)}$)

The Raman spectra of $(50\text{-}x/2)Na_2O - xCuO - (50\text{-}x/2)P_2O_5$ glasses (line I) show quite different shapes depending on the CuO content (Fig. 10). With increasing copper ions content in the $NaPO_3$ glass matrix, we observe that the intensity of the two peaks around ~ 684 and ~ 1162 cm^{-1} together with the band near ~ 1270 cm^{-1} found in metaphosphate glasses, as mentioned previously (Table 3), decreases until disappearing at $x \sim 25$. From $x = 25$ mol% (i.e. the triphosphate composition), the spectra completely change their shape; new bands at 633, 745 and ~ 1042 cm^{-1} occur and grow in intensity as the CuO content further increases. The last two ones are assigned respectively to the symmetric stretching vibration P-O-P and to the symmetric stretching mode of non-bridging oxygen $(PO_3)_{sym}$ ($Q^{(1)}$ species) in dimeric $(P_2O_7)^{4-}$ units. In other words, the introduction of a network modifier such as CuO into $NaPO_3$ glass causes the depolymerization of the glass structure made of the infinite phosphate chains leading to a distribution of shorter chain length species down to the dimeric diphosphate composition occurring at x = 0.33. These results are consistent with those previously reported for similar polyphosphate glassy systems [22], [23], [24], [31], [32] except that a well-defined band at 633 cm^{-1} is observed for $x \geq 0.25$. We assign this band at 633 cm^{-1} to the stretching like symmetric vibration of "square planar" $CuO_{4/2}$ structural units that are evidenced for the first time in phosphate glasses. The oxygen atoms involved in these groups may pertain to different PO_3 end groups of diphosphate anions, such as those existing in crystalline $Na_2CuP_2O_7$ under the form of $(CuP_2O_7)_\infty$ anionic ribbons [27]. Also CuO single crystals are formed by such $CuO_{4/2}$ interconnected structural units that exhibit a characteristic Raman active

symmetrical stretching-like mode at 630 cm^{-1}[33]. So, we conclude that a reticulation of the glass network is achieved by the creation of Cu–O–P bridges between diphosphate groups.

3.5. Diffuse reflectance study

Fig. 12, Fig. 13 show the diffuse reflectance spectra, recorded in the 250–750 cm^{-1} range, respectively for (50-*x*/2)Na_2O - *x*CuO - (50-*x*/2)P_2O_5 (line I) and (50-*x*)Na_2O - *x*CuO - 50P_2O_5 (line II) glasses. Both families of these glasses present comparable results; a broad visible transmission band for the low CuO content glasses, and a shouldered transmission by increasing the CuO amount with a more important transmission in the red range compared to the blue range. All the studied copper glasses revealed a total absorption in the UV and IR ranges. The transmission bands in the (50-*x*/2)Na_2O – *x*CuO – (50-*x*/2)P_2O_5 glasses ($0 \leq x \leq 40$; line I) are almost similar, with a high energy edge around 340 nm and a low energy edge near 600 nm. The increase of CuO concentration in the glass-matrix leads to the increase of the intensities of absorption in the 400–550 range, and the color of the glasses turns from a royal blue (for x = 10) into a darker blue as the CuO amount increases. The glasses with x > 30 present a dark green color, which is related to the increase of the overall absorption and the apparition of an additional absorption band in the blue range (< 450 nm).

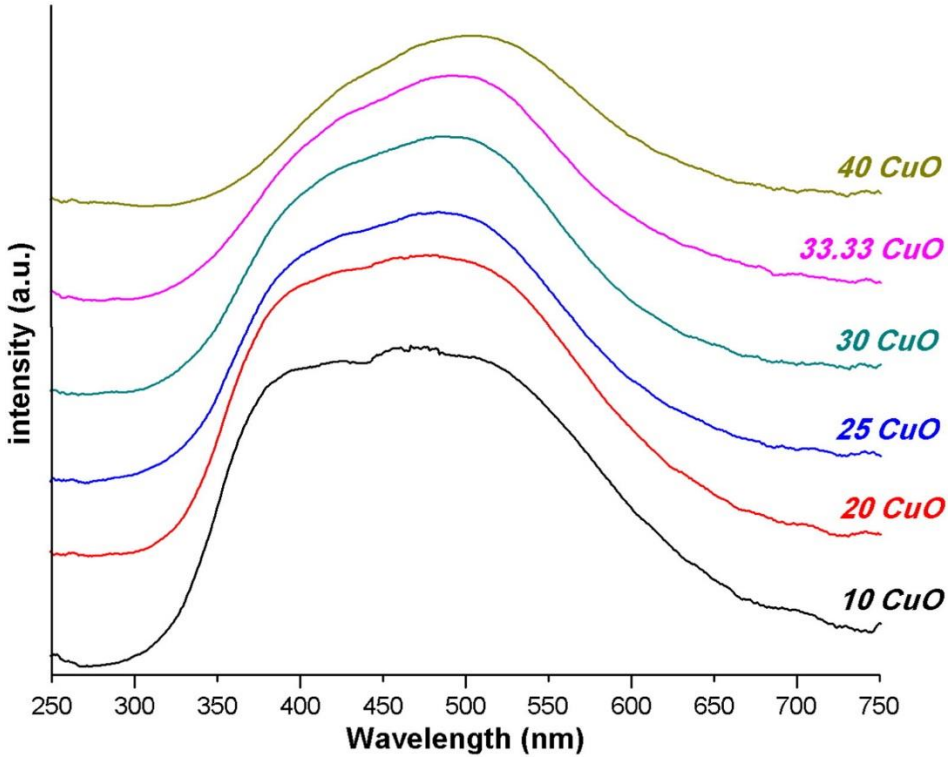

Fig. 12. UV – Vis diffuse reflectance spectra of (50-x/2) Na_2O – x CuO – (50- x/2) P_2O_5 ($0 < x \leq 40$) glasses.

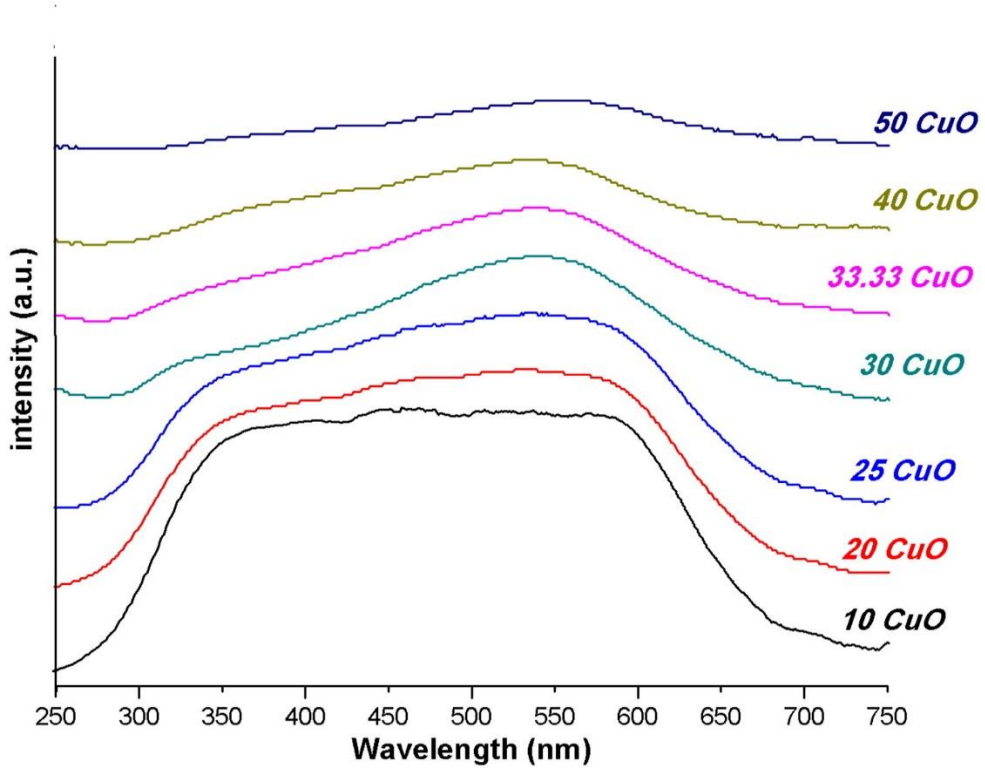

Fig. 13. UV – Vis diffuse reflectance spectra of (50-x)Na_2O – xCuO – 50P_2O_5 (0 < x ≤ 50) glasses.

The glasses from the (50-*x*)Na_2O – *x*CuO – 50P_2O_5 series (0 ≤ *x* ≤ 50; line II) present a quite different aspect. The first sample of this series (x = 10) shows a broad transmission band, from 300 nm to 700 nm, with a light blue color. With the introduction of copper oxide, the transmission band edges narrow as they shift to 320 nm for the high energy edge and to 650 nm for the low energy edge. The color of the glasses is similar to the first series one. The substitution of Na_2O by CuO induces a blue absorption and a maximum transmission at 540 nm, which corresponds to dark green glasses that gets darker as the CuO content increases.

It is known that copper takes an octahedral coordination. Thus, Cu^{2+} in vitreous state produces a ligand field splitting of the free ion energy level. A tetragonal distortion of the octahedral coordination of Cu^{2+} is induced by the Jahn-Teller effect due to the non-crystalline structural disorder [34]. This effect leads to an elongated tetragonal octahedral environment surrounding copper with four short bond lengths in the plane and two larger axial bond lengths. The splitting shifts then from octahedral to tetragonal, pyramid or square plane by increasing the crystal field.

The low energy absorption band located above 600 nm is attributed to the d-d electronic transition of Cu^{2+} ion [35]. It is also found that this band shifted toward high energies as the amount of CuO increased. This behavior can be explained by an emphasis of the distortion, which leads to an increase of the splitting energy of the corresponding 3d level [12]. The high energy band below 300 nm is attributed to the O⟶Cu charge transfer which corresponds to an electron transition between the 2p state of oxygen and the 3d state of copper [36]. As it can be seen easily in Fig. 14, the gap between the two energy states decreases while increasing the CuO amount, which leads also to an increase of the related wavelength. This behavior, observed in several glass systems containing transition metal oxides, is attributed to the structural change in the glass network and the formation of non-bridging oxygen bonds [37]. Optical measurements, in the 750–2000 cm^{-1} domain and EPR spectra will be carried out to have more information on the coordination of copper ions.

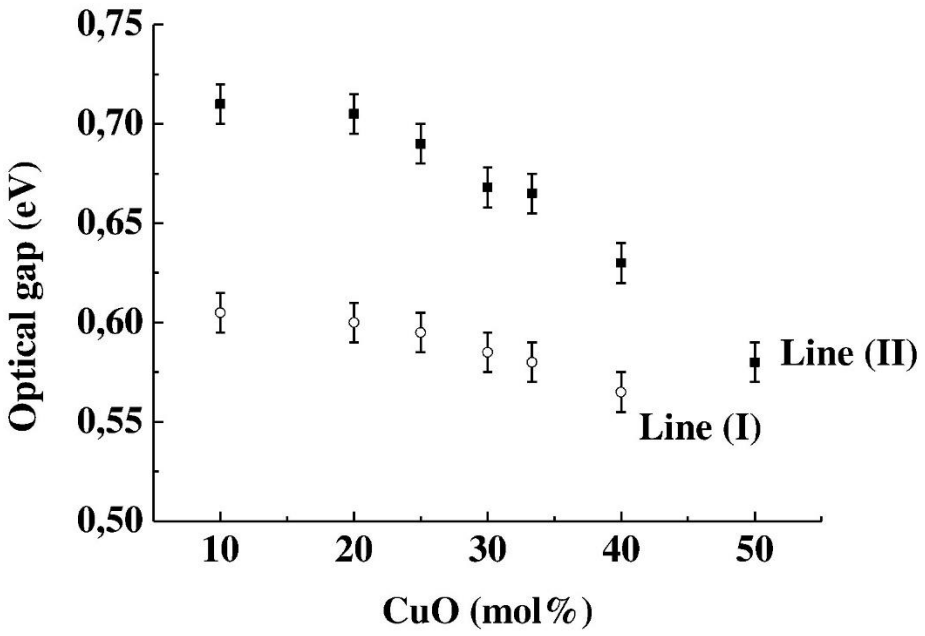

Fig. 14. Variation of optical band gap of (50-x/2)Na_2O – xCuO – (50-x/2)P_2O_5 (0 < x ≤ 40) (line I) and (50-x) Na_2O – x CuO – 50 P_2O_5 (0 < x ≤ 50) (line II) glasses.

3.6. Dissolution heat of glasses

Phosphate glasses are known to have a relatively poor chemical durability thus making them easily soluble in aqueous as well as acidic solutions. The microcalorimetric study undertaken consists on measuring dissolution heat of the different samples in a very specific solvent. The choice of the latter is determined by its ability to dissolve instantaneously the vitreous material without forming precipitates leading to thermochemical phenomena which will also be detected by the calorimeter and then interfere with the desired measurement. After many attempts of dissolving an amount of studied glasses in many inorganic solvents (such as: H_3PO_4, HNO_3, HCl), we observed that a 9% weight nitric acid (HNO_3) solution is the best convenient for our analysis. During the dissolution process, the volume of the solvent is fixed at 4.5 10^{-3} l of HNO_3 (9%weight), in both compartments of the micro-calorimeter, and the mass of different samples close to 20 mg. Complementary experiments were realized for both series of glasses in order to determine the relative error on the integrated area, using a statistical calculation method developed by Pattengill [21]. Table 4 reports the dissolution heat values of the investigated glasses. Fig. 15 shows the variation of the dissolution heat versus mol% of CuO for the two series of glasses.

Table 4
Molar dissolution heat for (50-*x*/2)Na_2O – *x*CuO – (50-*x*/2)P_2O_5 (0 ≤ *x* ≤ 40) and (50-*x*) Na_2O – *x*CuO – 50 P_2O_5 (0 ≤ *x* ≤ 50) glasses.

(50-x/2) Na_2O – x CuO – (50-x/2) P_2O_5		(50-x) Na_2O – x CuO – 50 P_2O_5	
Vitreous sample	Q_{diss} (kJ/mol)	Vitreous sample	Q_{diss} (kJ/mol)
x = 0	6.29 ± 0.03	*x = 0*	6.29 ± 0.03
x = 10	4.74 ± 0.02	*x = 10*	4.23 ± 0.16
x = 20	4.38 ± 0.02	*x = 20*	2.18 ± 0.09
x = 25	2.39 ± 0.01	*x = 25*	0.71 ± 0.03
x = 30	1.47 ± 0.01	*x = 30*	0.30 ± 0.01
x = 33.33	−2.30 ± 0.01	*x = 33.33*	−0.25 ± 0.01
x = 40	−8.65 ± 0.04	*x = 40*	−2.38 ± 0.09
–	–	*x = 50*	−3.77 ± 0.15

Dissolution heat decreases gradually from 6.29 ± 0.03 kJ/mol to − 8.65 ± 0.04 kJ/mol for (50-*x*/2) Na_2O – *x*CuO – (50-*x*/2) P_2O_5 glasses and to − 3.8 ± 0.2 kJ/mol for (50-*x*) Na_2O – *x*CuO – 50 P_2O_5 glasses. It is seen from these results that the dissolution phenomenon is endothermic for glasses with low content in CuO (x < 30) and exothermic for glasses rich in CuO. This change agrees well with the different measurements (T_g, density) made previously. Indeed we observed a strong modification in many properties around 30 mol% CuO. The evolution of the dissolution heat of Na_2O-CuO-P_2O_5 glasses from endothermic to exothermic phenomenon is due to the modification of the vitreous network when CuO replaces Na_2O. We can see that the dissolution heat is endothermic for glasses with weak bonds (–Na–O–P– linkages) and exothermic for glasses with strong bonds (–Cu–O–P– linkages). The decrease in the dissolution heat in acid solution shows a dependence of this quantity with the increasing covalent bonds in the network. These results are similar to those reported previously for Na_2O-MO-P_2O_5 glasses (M═Zn, Mn, Mg, Sr) [22], [23], [24], [25].

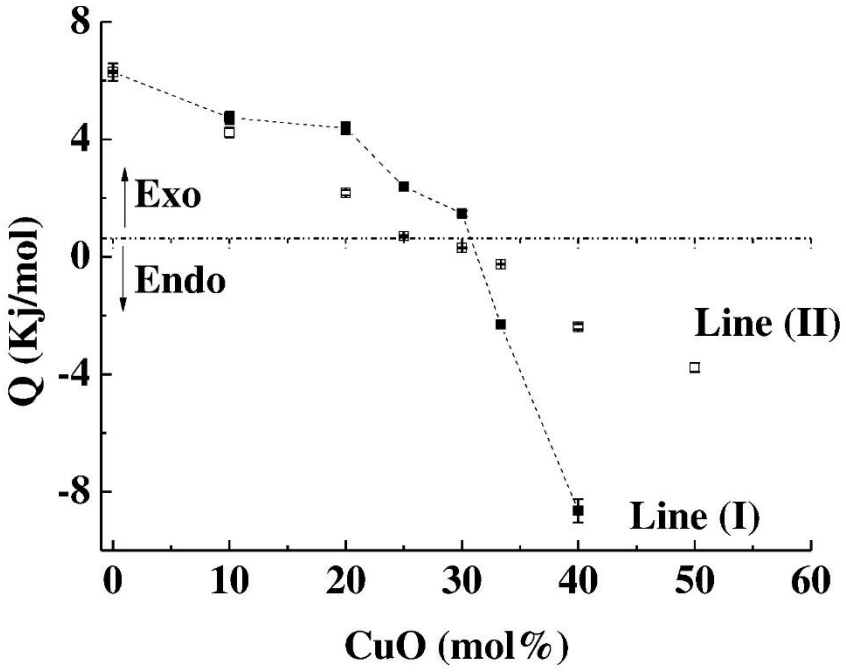

Fig. 15. Evolution of dissolution heat quantities of (50-x/2)Na_2O–xCuO–(50-x/2)P_2O_5 ($0 \leq x \leq 40$) (line I) and (50-x)Na_2O–xCuO–50P_2O_5 ($0 \leq x \leq 50$) (line II) versus CuO content. The line is drawn as guide to the eyes.

4. Conclusions

The role of the copper oxide CuO was investigated for two glass series of the ternary system Na_2O–CuO–P_2O_5, using various techniques: density measurements, DSC, XRD, Raman and diffuse reflectance. The evolution of density, molar volume and glass transition temperature versus CuO content implies the reticulation of the glass network due to the replacement of Na—O bonds by the more covalent Cu–O bonds for both series of glasses. These results were confirmed by the Raman and reflectance diffuse spectroscopy studies. Indeed the reticulation of the glass network is achieved by the creation of Cu–O–P linkages. All results were correlated with dissolution heat measurements by micro-calorimetry. The dissolution enthalpy decreases, for both series, when the CuO content increases. This study showed also a transition between an endothermic behavior of the glass dissolution, observed for the glasses with lower CuO content, and an exothermic phenomenon that occurs around 30–33 mol% CuO, corresponding to an important modification of the vitreous network.

Acknowledgements

The authors acknowledge the Morocco-France cooperation (Volubilis Program MA/120/229) and AUF (PCSI 59113PS024) for the financial support.

References

1. N.M. Shash, F.E. Salman, M.K. El-Mansy, H.A. Ghodair. **Influence of lithium phosphate concentration and temperature on the electrical conduction of $(76V_2O_5–24P_2O_5)_{1-x}(Li_3PO_4)_x$ glasses.** J. Phys. Chem. Solids, 65 (2004), pp. 891-900, 10.1016/j.jpcs.2003.09.030
2. J.A. Wilder. **Glasses and glass ceramics for sealing to aluminum alloys.** J. Non-Cryst. Solids, 38 & 39 (1980), pp. 879-884, 10.1016/0022-3093(80)90548-7
3. S.M. Hsu, S.W. Yung, R.K. Brow, W.L. Hsu, C.C. Lu, F.B. Wu, *et al.* **Effect of silver concentration on the silver-activated phosphate glass.** Mater. Chem. Phys., 123 (2010), pp. 172-176, 10.1016/j.matchemphys.2010.03.078
4. J.H. Campbell, T.I. Suratwala. **Nd-doped phosphate glasses for high-energy/high-peak-power lasers.** J. Non-Cryst. Solids, 263-264 (2000), pp. 318-341, 10.1016/S0022-3093(99)00645-6
5. Y. Abe, H. Shimakawa, L.L. Hench. **Protonic conduction in alkaline earth metaphosphate glasses containing water.** J. Non-Cryst., 51 (1982), pp. 357-365, 10.1016/0022-3093(82)90156-9
6. T. Gilchrist, M.A. Glasby, D.M. Healy, G. Kelly, D.V. Lenihan, K.L. McDowall, *et al.* **In vitro nerve repair–in vivo. The reconstruction of peripheral nerves by entubulation with biodegradeable glass tubes–a preliminary report.** Br. J. Plast. Surg., 51 (1998), pp. 231-237, 10.1054/bjps.1997.0243
7. Ahmed, M. Lewis, I. Olsen, J.C. Knowles. **Phosphate glasses for tissue engineering: part 1. Processing and characterisation of a ternary-based P_2O_5–CaO–Na_2O glass system.** Biomaterials, 25 (2004), pp. 491-499, 10.1016/S0142-9612(03)00546-5
8. Ahmed, M. Lewis, I. Olsen, J.C. Knowles. **Phosphate glasses for tissue engineering: part 2. Processing and characterisation of a ternary-based P_2O_5–CaO–Na_2O glass fibre system.** Biomaterials, 25 (2004), pp. 501-507, 10.1016/S0142-9612(03)00547-7
9. M. Uo, M. Mizuno, Y. Kuboki, A. Makishima, F. Watari. **Properties and cytotoxicity of water soluble Na_2O-CaO-P_2O_5 glasses.** Biomaterials, 19 (1998), pp. 2277-2284, 10.1016/S0142-9612(98)00136-7
10. T. Minami, J.D. Mackenzie. **Thermal expansion and chemical durability of phosphate glasses.** J. Am. Ceram. Soc., 60 (1977), pp. 232-235, 10.1111/j.1151-2916.1977.tb14113.x
11. R.K. Brow. **Review: the structure of simple phosphate glasses.** J. Non-Cryst. Solids, 263 (2000), pp. 1-28, 10.1016/S0022-3093(99)00620-1
12. T. Maekawa, T. Yokokawa, K. Niwa. **Optical spectra of transition metals in Na_2O-P_2O_5 glasses.** Bull. Chem. Soc. Jpn., 42 (1969), pp. 2102-2106, 10.1246/bcsj.42.2102
13. P.Y. Shih, S.W. Yung, T.S. Chin. **Thermal and corrosion behavior of P_2O_5-Na_2O-CuO glasses.** J. Non-Cryst. Solids, 224 (1998), pp. 143-152, 10.1016/S0022-3093(97)00460-2
14. P.Y. Shih. **FTIR and XPS studies of P_2O_5 - Na_2O - CuO glasses.** J. Non-Cryst. Solids, 244 (1999), pp. 211-222, 10.1016/S0022-3093(99)00011-3
15. P.Y. Shih, T.S. Chin. **Effect of redox state of copper on the properties of P_2O_5 - Na_2O - CuO glasses.** Mater. Chem. Phys., 60 (1999), pp. 50-57, 10.1016/S0254-0584(99)00070-X
16. P.Y. Shih, J.Y. Ding, S.Y. Lee. **^{31}P MAS-NMR and FTIR analyses on the structure of CuO-containing sodium poly- and meta-phosphate glasses.** Mater. Chem. Phys., 80 (2003), pp. 391-396, 10.1016/S0254-0584(03)00098-1
17. Chahine, M. Et-tabirou, M. Elbenaissi, M. Haddad, J.L. Pascal. **Effect of CuO on the structure and properties of $(50 – x/2)Na_2O$-xCuO-$(50 – x/2)P_2O_5$ glasses.** Mater. Chem. Phys., 84 (2004), pp. 341-347, 10.1016/j.matchemphys.2003.11.009

18. S. Daoudi, L. Bejjit, M. Haddad, M.E. Archidi, A. Chahine, M. Et-tabirou, P. Molinié. **EPR and magnetic susceptibility of $Na_2O–CuO–P_2O_5$ glasses.** Spectrosc. Lett., 40 (5) (2007), pp. 785-795, 10.1080/00387010701521900

19. K. Brahim, I. Khattech, J.P. Dubès, M. Jemal. **Etude cinétique et thermodynamique de la dissolution de la fluorapatite dans l'acide phosphorique.** Thermochim. Acta, 436 (2005), pp. 43-50, 10.1016/j.tca.2005.06.019

20. H. Zendah, I. Khattech, M. Jemal. **Synthesis, characterization and thermochemistry of acid attack of "B" type carbonate fluorapatites.** J. Therm. Anal. Calorim., 109 (2012), pp. 855-861, 10.1007/s10973-011-1858-1

21. M.E. Pattengill, D.E. Sands. **Statistical significance of linear least-squares parameters.** J. Chem. Educ., 56 (1979), pp. 244-247, 10.1021/ed056p244

22. R. Oueslati, S. Krimi, J.J. Videau, I. Khattech, A. El Jazouli, M. Jemal. **Structural and thermochemical study of $Na_2O–ZnO–P_2O_5$ glasses.** J. Non-Cryst. Solids, 390 (2014), pp. 5-12, 10.1016/j.jnoncrysol.2014.02.020

23. R.O. Omrani, S. Krimi, J.J. Videau, I. Khattech, A. El Jazouli, M. Jemal. **Structural investigations and calorimetric dissolution of manganese phosphate glasses.** J. Non-Cryst. Solids, 389 (2014), pp. 66-71, 10.1016/j.jnoncrysol.2014.02.006

24. R. Oueslati Omrani, A. Kaoutar, A. El Jazouli, S. Krimi, I. Khattech, M. Jemal. **Structural and thermochemical properties of sodium magnesium phosphate glasses.** J. Alloys Compd., 632 (2015), pp. 766-771, 10.1016/j.jallcom.2015.01.297

25. M.A. Cherbib, S. Krimi, A. El Jazouli, I. Khattech, L. Montagne, B. Revel, M. Jemal. **Structural and thermochemical study of strontium sodium phosphate glasses.** J. Non-Cryst. Solids, 447 (2016), pp. 59-65, 10.1016/j.jnoncrysol.2016.05.025

26. H.M. Ondik. **The structure of anhydrous sodium trimetaphosphate $Na_3P_3O_9$ and the monohydrate $Na_3P_3O_9$, H_2O.** Acta Cryst., 18 (1965), pp. 226-232, 10.1107/S0365110X65000518

27. K.M.S. Etheredge, S. Hwu. **Synthesis of a new layered sodium copper (II) pyrophosphate, $Na_2CuP_2O_7$, via an eutectic halide flux.** Inorg. Chem., 34 (1995), pp. 1495-1499, 10.1021/ic00110a030

28. M. Laügt, I. Tordjman, J.C. Guitel, G. Bassi. **Structure cristalline du polyphosphate de cuivre-sodium $CuNa_2(PO_3)_4$.** Acta Cryst. B28 (1972), pp. 2721-2725, 10.1107/S0567740872006843

29. J. Massera, K. Bourhis, L. Petit, M. Couzi, L. Hupa, M. Hupa, J.J. Videau, T. Cardinal. **Effect of glass composition on the chemical durability of zinc-phosphate-based glasses in aqueous solutions.** J. Phys. Chem. Solids, 74 (2013), pp. 121-127, 10.1016/j.pcs.2012.08.010

30. M. Laügt, J.C. Gitel, I. Tordjman, G. Bassi. **La structure crystalline du tétramétaphosphate de cuivre $Cu_2P_4O_{12}$.** Acta Cryst., B28 (1972), pp. 201-208, 10.1107/S0567740872002079

31. E. Metwalli, M. Karabulut, D.L. Sidebottom, M.M. Morsi, R.K. Brow. **Properties and structure of copper ultraphosphate glasses.** J. Non-Cryst. Solids, 344 (2004), pp. 128-134, 10.1016/j.jnoncrysol.2004.07.058

32. L. Ma, R.K. Brow, A. Choudhury. **Structural study of $Na_2O–FeO–Fe_2O_3–P_2O_5$ glasses by Raman and Mössbauer spectroscopy.** J. Non-Cryst. Solids, 402 (2014), pp. 64-73, 10.1016/j.jnoncrysol.2014.05.013

33. H.F. Goldstein, D. Kim, P.Y. Yu, L.C. Bourne, J.P. Chaminade, L. Nganga. **Raman study of CuO single crystal.** Phys. Rev. B., 41 (1990), pp. 7192-7194, 10.1103/PhysRevB.41.7192

34. R.V.S.S.N. Ravikumar, V.R. Reddy, V. Chandrasekhar, B.J. Reddy, Y.P. Reddy, P.S. Rao. **Tetragonal site of transition metal ions doped sodium phosphate glasses.** J. Alloys Compd., 337 (2002), pp. 272-276, 10.1016/S0925-8388(01)01963-6

35. S.P. Singh, A. Tarafder. **Comparative investigation on the effect of alkaline earth oxides on the intensity of absorption bands due to Cu^{2+}, Mn^{3+} and Cr^{3+} ions in ternary silicate glasses.** Bull. Mater. Sci., 27 (2004), pp. 281-287, 10.1007/BF02708518

36. B.-S. Bae, M.C. Weinberg. **Ultraviolet optical absorptions of semiconducting copper phosphate glasses.** J. Appl. Phys., 73 (1993), p. 7760, 10.1063/1.353975

37. M.A. Ouis, H.A. ElBatal, A.M. Abdelghany, A.H. Hammad. **Structural and optical properties of CuO in zinc phosphate glasses and effects of gamma irradiation.** J. Mol. Struct., 1103 (2016), pp. 224-231